Molecular Biology of the Cell
Vol. 21, 4240–4250, December 1, 2010

Hepatocyte Growth Factor Inhibits Apoptosis by the Profibrotic Factor Angiotensin II via Extracellular Signal-regulated Kinase 1/2 in Endothelial Cells and Tissue Explants

Young H. Lee, Ana P. Marquez, Ognoon Mungunsukh, and Regina M. Day

Department of Pharmacology, Uniformed Services University of the Health Sciences, Bethesda, MD 20814

Submitted April 22, 2010; Revised September 3, 2010; Accepted September 23, 2010
Monitoring Editor: J. Silvio Gutkind

Hepatocyte growth factor (HGF), an endogenous tissue repair factor, attenuates apoptosis in many primary cell types, but the mechanism is not completely understood. Our laboratory demonstrated that angiotensin (Ang) II activates the intrinsic apoptotic pathway in primary endothelial cells (ECs) via reduction of the antiapoptotic protein Bcl-x_L. Ang II decreased Bcl-x_L mRNA half-life by reducing its binding to nucleolin, a protein that normally binds a 3′ AU-rich region and stabilizes Bcl-x_L mRNA. We hypothesized HGF may block apoptosis induced by Ang II. We used primary EC and ex vivo cultures of rat lung tissue to investigate HGF inhibition of Ang II-induced apoptosis. Our data indicated HGF abrogated Ang II-induced apoptosis by inhibiting cytochrome *c* release, caspase-3 activation, and DNA fragmentation. RNA-immunoprecipitation experiments demonstrated that HGF stabilized Bcl-x_L mRNA by increasing nucleolin binding to the 3′-untranslated region that was associated with cytoplasmic localization of nucleolin. Cytoplasmic localization of nucleolin and Bcl-x_L mRNA stabilization required HGF activation of extracellular signal-regulated kinase (ERK)1/2, but not phosphatidylinositol 3-kinase. HGF also blocked Ang II-induced caspase-3 activation and lactate dehydrogenase release in tissue explants in an ERK-dependent manner.

INTRODUCTION

Hepatocyte growth factor (HGF) was originally identified as a potent mitogen for mature hepatocytes but has since been demonstrated to exert potent motogenic, mitogenic, and morphogenic activities in cells of epithelial and endothelial origin (Rubin *et al*., 1993). HGF activity plays a critical role in embryogenesis and organogenesis, but in the adult HGF functions in a variety of organs as a tissue repair factor (Matsumoto and Nakamura, 1993; Rubin *et al*., 1993). HGF promotes normal repair and prevents aberrant wound healing in several organ systems, including the lung, heart, kidney, and liver (Matsumoto and Nakamura, 1993; Kawaida *et al*., 1994; Kosai *et al*., 1999; Dohi *et al*., 2000; Kitta *et al*., 2001). Animal studies show that administration of HGF induces proliferation of epithelial and endothelial cells and is believed to contribute to normal tissue regeneration. The simultaneous or delayed administration of HGF protein to mice with bleomycin-induced lung injury was demonstrated to block fibrotic remodeling, including the prevention of epithelial cell apoptosis, the inhibition of fibroblast foci, and the inhibition of collagen accumulation (Yaekashiwa *et al*., 1997; Dohi *et al*., 2000). Ectopic expression of HGF, using either adenoviral expression or in vivo plasmid transient transfection, also was shown to inhibit bleomycin-induced lung remodeling (Ebina *et al*., 2002; Watanabe *et al*., 2005).

Met, the HGF receptor, is a tyrosine kinase receptor with a single transmembrane domain. HGF binding to Met induces phosphorylation in the tyrosine kinase domain as well as in a carboxy-terminal multifunctional docking domain, the site of activation of downstream signaling pathways (Ponzetto *et al*., 1994). Among the pathways activated by HGF are the extracellular signal-regulated kinase (ERK)1/2 mitogen-activated protein kinase (MAPK) and the phosphatidylinositol 3-kinase (PI3K)/Akt pathways, both associated with cellular survival and growth (Brunet *et al*., 1999; Day *et al*., 1999; Lee *et al*., 2008). The activation of cell survival and proliferation is thought to be critical for the antifibrotic functions of HGF (Kitta *et al*., 2001; Matsumoto and Nakamura, 2001).

Angiotensin (Ang) II was first studied for its role in blood pressure homeostasis but has more recently been shown to play a key role in fibrosis of lung, liver, kidney, and heart (Konigshoff *et al*., 2007; Wynn, 2008). Ang II is believed to play a dual role in the progression of dysfunctional wound repair by promoting the apoptosis of tissue epithelial and endothelial cells as well as inducing the growth and transdifferentiation of myofibroblasts (Filippatos *et al*., 2001; Marshall *et al*., 2004). Local synthesis of Ang II has been observed

This article was published online ahead of print in *MBoC in Press* (http://www.molbiolcell.org/cgi/doi/10.1091/mbc.E10–04–0341) on October 6, 2010.

Address correspondence to: Regina M. Day (rday@usuhs.mil).

Abbreviations: Ang, angiotensin; BSA, bovine serum albumin; EC, endothelial cell; ERK, extracellular signal-regulated kinase; FBS, fetal bovine serum; HGF, hepatocyte growth factor; PI3K, phosphatidylinositol 3-kinase; UTR, untranslated region.

in fibrotic plaques, and human myofibroblasts from patients with idiopathic pulmonary fibrosis were found to generate Ang II (Wang *et al*., 1999a). Furthermore, the inhibition of Ang II signaling was associated with the reduction of epithelial and endothelial cell apoptosis in an animal model of pulmonary fibrosis (Wang *et al*., 2000). Studies showed that Ang II induced apoptosis via the intrinsic apoptotic pathway in lung epithelial cells (Wang *et al*., 1999b).

Our laboratory recently demonstrated that Ang II activates the intrinsic apoptotic pathway in primary endothelial cells (ECs), including the release of cytochrome *c*, the activation of caspase-3, and caused DNA laddering (Lee *et al*., 2010). Ang II treatment of ECs resulted in the loss of Bcl-x_L protein through the destabilization of its mRNA. We found that Ang II induced Src homology 2 domain-containing protein tyrosine phosphatase- (SHP-2-) dependent nuclear translocation of nucleolin, thus preventing its binding to the Bcl-x_L mRNA 3′-untranslated region (UTR), leading to Bcl-x_L mRNA instability and degradation and allowing the activation of the intrinsic apoptotic pathway.

Here, we examined the effects of HGF on Ang II-induced apoptosis in primary cultures of ECs. HGF inhibited the release of cytochrome *c* and activation of caspase-3 in response to Ang II. HGF protected the Bcl-x_L mRNA from Ang II-induced degradation in an ERK1/2-mediated nucleolin-dependent pathway. Together, these data suggest that HGF protects endothelial cells against Ang II-induced apoptosis via activated ERK1/2-mediated cytoplasmic localization of nucleolin that stabilizes Bcl-x_L mRNA, thus inhibiting the intrinsic apoptotic pathway.

MATERIALS AND METHODS

Reagents

Angiotensin II was purchased from Bachem (Torrance, CA). Antibodies against cytochrome *c* and β-actin were purchased from Santa Cruz Biotechnology (Santa Cruz, CA); anti-cleaved caspase-3 was purchased from Cell Signaling Technology (Danvers, MA). The *Renilla*-Bcl-x_L construct was the gift of Dr. Tim Bowden (University of Arizona, Tucson, AZ; Zhang *et al*., 2008a). Purified human HGF was the gift of Dr. G. F. Vande Woude (Van Andel Research Institute, Grand Rapids, MI). Dominant-negative Ras in an adenoviral expression vector was provided by Dr. M. L. Cutler (Uniformed Services University of the Health Sciences, Bethesda, MD). Constitutively active and dominant-negative (DN) mitogen-activated protein kinase kinase (MEK) 1 in an adenoviral expression vector was the gift of Dr. Y. J. Suzuki (Georgetown University, Washington, DC).

Cell Culture

Bovine pulmonary artery ECs were purchased from American Type Culture Collection (Manassas, VA). Passages 2–8 cells were used for all experiments and were cultured in RPMI 1640 medium (Invitrogen, Carlsbad, CA) containing 10% fetal bovine serum (FBS) (Gemini Bioproducts, Woodland, CA), 1% penicillin/streptomycin, and 0.5% Fungizone (Invitrogen). Cells were grown in 5% CO_2 at 37°C in a humidified atmosphere in a culture incubator.

Cell Lysate

Cells were washed with ice-cold phosphate-buffered saline (PBS) and lysed in 50 mM HEPES, pH 7.4, 1% (vol/vol) Triton X-100, 4 mM EDTA, 1 mM sodium fluoride, 0.1 mM sodium orthovanadate, 1 mM tetrasodium pyrophosphate, 2 mM phenylmethylsulfonyl fluoride, 10 μg/ml leupeptin, and 10 μg/ml aprotinin. Lysates were incubated 15 min on ice and then vortexed; insoluble materials were removed by centrifugation (14,000 × *g* for 10 min at 4°C). For immunoprecipitation of Bax, cells were washed with cold PBS and lysed in 3-[(3-cholamidopropyl)dimethylammonio]propanesulfonate (CHAPS) buffer [50 mM Tris-HCl, 1 mM EGTA, 1% (wt/vol) CHAPS, 10% glycerol, 50 mM sodium fluoride, 1 mM sodium orthovanadate, 2 mM phenylmethylsulfonyl fluoride, 10 μg/ml leupeptin, and 10 μg/ml aprotinin]. Equal concentrations of protein from cell lysates were incubated with primary antibody (1:1000 dilution). GammaBind Plus beads (1:100 dilution; GE Healthcare, Little Chalfont, Buckinghamshire, United Kingdom) were added and samples were rotated at 4°C overnight. The beads were centrifuged at 10,000 × *g* for 10 min at 4°C and washed twice with lysis buffer containing protease and phosphatase inhibitors. To elute, beads were resuspended in 25 μl of Laemmli buffer incubated for 5 min at 95°C.

Western Blots

Whole cell lysates (10 μg of total protein) were subjected to SDS-polyacrylamide gel electrophoresis and electroblotted onto nitrocellulose membrane. Membranes were blocked with 5% bovine serum albumin (BSA) in Tween 20/Tris-buffered saline (TTBS) for 1 h at ambient temperature. Membranes were then incubated overnight at 4°C with primary antibody (1:1000 dilution) in TTBS containing 0.5% (wt/vol) BSA. Membranes were washed three times with TTBS for 10 min, followed by incubation with horseradish peroxidase-labeled secondary antibody (1:1000 in TTBS) for 1 h at ambient temperature. For protein detection, membranes were washed for 3 h with TBS, incubated in ECL solution (Pierce Chemical, Rockford, IL), and analyzed on a LAS-1000Pro image reader (FujiFilm USA, Valhalla, NY).

Mitochondria and Mitochondria-free Cytosolic Protein Extraction

Mitochondria extraction was performed using the mitochondria isolation kit for cultured cells according to the manufacturer's protocol (Pierce Chemical).

Neutral Comet Assay

The neutral comet assay was used to measure double-stranded DNA breaks as an indication of apoptosis (Lee *et al*., 2010). After treatment, cells were embedded in 1% (wt/vol) low-melting agarose and placed on comet slides (Trevigen, Gaithersburg, MD). Slides were placed in lysis solution (2.5 M NaCl, 1% Na-lauryl sarcosinate, 100 mM EDTA, 10 mM Tris base, and 0.01% Triton X-100) for 30 min, followed by a wash in 1× Tris borate-EDTA (TBE) buffer (0.089 M Tris, 0.089 M boric acid, and 0.002 M EDTA, pH 8.0). Nuclei were electrophoresed for 10 min at 18 V in 1× TBE. Cells were then fixed with 75% ethanol for 10 min and air-dried overnight, stained with 1× SYBR Green (Invitrogen) or propidium iodide (Sigma-Aldrich, St. Louis, MO), and visualized with an FV500 confocal laser scanning microscope (Olympus Imaging America, Center Valley, PA) by using 20× magnification at 478 nm excitation, 507 nm emission wavelengths for SYBR Green and at 535 nm excitation, 617 nm emission wavelengths for propidium iodide. All cells were counted in randomly selected fields for each treatment group and assigned into type A, B, or C comet categories, based on their tail moments. Type C comets were defined as apoptotic cells (Krown *et al*., 1996).

DNA Laddering Assay

Cells were harvested in the medium and pelleted at 1000 × *g*. Pellets were resuspended and incubated on ice in lysis buffer (1× Tris-EDTA and 0.2% Triton, pH 8.0) for 15 min. Resuspended pellet was centrifuged (14,000 × *g* for 10 min at 4°C), and supernatant containing the fragmented DNA was collected. RNase A (final concentration, 60 mg/ml) was added and incubated for 30 min at 37°C. SDS was added to a final concentration of 0.5% along with 150 μg/ml proteinase K and incubated 2 h at 50°C. Then, 0.1 volume of 5 M NaCl and 1 volume of ice cold isopropanol were added, and samples were incubated on ice for 10 min. The samples were centrifuged at 13,000 × *g* for 15 min at 4°C. The DNA pellet was briefly dried and dissolved in 20 μl of TE buffer, followed by electrophoresis (~2 h at 20 V) in 1.5% agarose.

RNA Isolation and Reverse Transcription (RT)

Total RNA was obtained from bovine ECs by using the RNeasy kit (QIAGEN, Valencia, CA). Genomic DNA was removed using the RNase-Free DNAse set (QIAGEN). RNA concentrations were determined spectroscopically at 260 nm (ND-1000 spectrophotometer; NanoDrop, Wilmington, DE). RNA (1.0 μg) was subjected to RT with GeneAmp RNA polymerase chain reaction (PCR) kit according to the manufacturer's protocol (Applied Biosystems, Foster City, CA).

Semiquantitative RT-PCR

We used 1 μl of cDNA from the RT reaction for the PCR reaction containing 0.4 μM each forward and reverse primer, 200 μM each dNTP, 1 U of i*Taq* DNA polymerase, and 1× PCR buffer (Bio-Rad Laboratories, Hercules, CA). The PCR primers for Bcl-x_L mRNA were as follows: 5′-GGT ATT GGT GAG TCG GAT CG and 5′-GCT GCA TTG TTC CCG TAG AG. PCR reactions were optimized for annealing temperatures using a temperature gradient in an iCycler (Bio-Rad Laboratories). Reactions were carried out for 25 cycles by using the following conditions: 95°C 1 min, 60°C 45 s, and 72°C 1.5 min. The last cycle extension was for 10 min at 65°C. PCR primers for glyceraldehyde-3-phosphate dehydrogenase (GAPDH) were as follows: 5′-GAA GCT CGT CAT CAA TGG AAA and 5′-CCA CTT GAT GTT GGC AGG AT. PCR reactions were analyzed on a 1.5% agarose gel in Tris EDTA buffer, and bands were visualized using ethidium bromide.

Determination of mRNA Half-Life

Bovine ECs were treated as indicated above and then incubated with 5 μg/ml actinomycin D for time courses between 30 min and 8 h. Total RNA was isolated and the level of Bcl-x_L mRNA was determined by quantitative PCR or by semiquantitative RT-PCR (primers listed above). Levels of GAPDH mRNA were determined by gel electrophoresis and used for normalization of the semiquantitative RT-PCR (primers are listed above). ImageJ software (http://www.uhnresearch.ca/facilities/wcif/index.htm) was used for quantification.

Plasmid Transfection

One day before transfection, cells were plated at 1.4×10^5 cells/well in a 12-well plate. DNA (1 μg/well) was transfected using the FuGENE 6 transfection reagent (Roche Applied Science, San Francisco, CA), according to the manufacturer's instructions, in serum-free, antibiotic-free medium. For luciferase assays, transfection mixtures contained a ratio of *Renilla*-Bcl-x_L reporter construct to luciferase control vector (RSV-Luc) of 6:1 to normalize transfection efficiency.

Dual-Luciferase Assay

Transfected cells were washed twice with cold PBS, lysed with passive lysis buffer, and assayed for firefly and *Renilla* luciferase activities using the dual-luciferase assay (Promega, Madison, WI) according to the manufacturer's instructions in a TD-20/20 luminometer (Turner Designs, Sunnyvale, CA).

RNA-Immunoprecipitation (IP)

Cells were harvested by centrifugation at 1000 $\times$ *g* for 3 min and resuspended in 10 ml of PBS. RNA and protein complexes were cross-linked by adding of 1.0% (vol/vol), final concentration, of formaldehyde and incubation at room temperature for 10 min with gentle mixing. Cross-linking was quenched by addition of glycine (pH 7.0; 0.125 mol/l, final concentration) at room temperature for 5 min. Cells were washed twice with 10 ml of PBS containing protease and RNAse inhibitors. The pellet was resuspended in 0.2 ml of NP-40 buffer [5 mM piperazine-*N*,*N*′-bis(2-ethanesulfonic acid), pH 8.0, 85 mM KCl, 0.5% NP-40, protease inhibitors, and RNase inhibitor] and incubated on ice for 10 min. Nuclei were pelleted by centrifugation at 1400 $\times$ *g* for 5 min at 4°C. Supernatant was sonicated three times for 20 s each at output level 6 of a sonic model 100 dismembrator (Thermo Fisher Scientific, Waltham, MA). The samples were cleared by centrifugation at 14,000 rpm for 10 min at 4°C and diluted 10-fold into IP buffer (0.01% SDS, 1.1% Triton X-100, 1.2 mM EDTA, 16.7 mM Tris, pH 8.1, 167 mM NaCl, protease inhibitors, and RNase inhibitor) to a final volume of 1 ml per immunoprecipitation reaction. A 1% aliquot was preserved as an input sample. Nucleolin antibody (1:1000 dilution) was added to each tube, and immune complexes were allowed to form by gentle mixing on a rotating platform at 4°C overnight. To collect immune complexes, 50 μl of Sepharose beads was added and mixed gently for 2 h followed by centrifugation at 60 $\times$ *g* for 2 min at 4°C. The immune complexes were washed for 5 min each with low salt (0.1% SDS, 1% Triton X-100, 2 mM EDTA, 20 mM Tris-HCl, pH 8.1, and 150 mM NaCl), high salt (0.1% SDS, 1% Triton X-100, 2 mM EDTA, 20 mM Tris-HCl, pH 8.1, and 500 mM NaCl), LiCl (0.25M LiCl, 1% NP-40, 1% deoxycholate, 1 mM EDTA, and 10 mM Tris-HCl. pH 8.1), and twice with TE buffer. Each wash was followed by 60 $\times$ *g* centrifugation for 1 min. Immune complexes were eluted in 500 μl of elution buffer (1% SDS, 0.1 M $NaHCO_3$, and RNase inhibitor). NaCl was added to a final concentration of 200 mM, and then samples were placed at 65°C for 2 h to reverse cross-linking. Next, 20 μl of 1 M Tris-Cl, pH 6.5, 10 μl of 0.5 M EDTA, and 20 μg of proteinase K were added to each sample and incubated at 42°C for 45 min. RNA was extracted using phenol:chloroform with glycogen as a DNA-carrier. DNA was removed with DNase (QIAGEN). RT-PCR was performed using 1 μl of the cDNA reaction for 25 cycles: denaturing was performed at 95°C for 1 min, annealing for 45 s at 60°C, and polymerase reaction for 1.5 min at 72°C. Primers were as follows: Bcl-x_L ARE-2, 5′-ACC TTC CTC AAT TGT CGT GG-3′ and 5′-GGG GAA AAG GGT CAG AAA C-3′; and Bcl-2 ARE, 5′-TGC TTT TGA GGA GGG CTG CAC and 5′-ACT GCC TGC CAC AGA CCA GC.

Ex Vivo Lung Explants

All treatment of animals was according to National Institutes of Health, Department of Defense, and institutional guidelines. Sprague Dawley rats (Taconic Farms, Germantown, NY) were housed one female with litter per cage in a facility accredited by the Association for Assessment and Accreditation of Laboratory Animal Care International. Animal rooms were maintained at 21 $\pm$ 2°C, 50 $\pm$ 10% humidity, and 12-h light/dark cycle. Commercial rodent ration (Harlan Teklad Rodent Diet 8604; Harlan, Indianapolis, IN) and water were freely available. Rat pups were obtained on postnatal day 10 or 11. Animals were anesthetized with pentobarbital and decapitated, or killed with Fatal-Plus. The surface of the anterior chest wall and upper abdomen were sterilized with 70% ethanol. After the trachea was exposed, a small nick was made to insert a 22-gauge needle with a short piece of polyethylene tube attached. Through a midline abdominal incision the chest cavity was exposed and the animal was exsanguinated by severing the abdominal aorta. The right ventricle was punctured and the lungs were perfused with sterile PBS to remove the blood. The trachea, lungs, and the heart were then aseptically dissected from the animal.

To obtain lung slices for the ex vivo culture, the lungs were inflated with 1% low melting point agarose dissolved in RPMI 1640 medium. The agarose was instilled via the trachea by using a syringe to fully inflate the lungs. The lung-heart blocks were placed in sterile cell culture plates at 4°C for at least 30 min to solidify the agarose. The heart was then excised from the lung, and each lobe of the lung was embedded on a cutting board with 1% agarose to prevent movement. The agarose-filled and embedded lungs were then cut into 500-μm-thick slices with a MclLwain tissue chopper (Geneq, Anjou, QC, Canada). Slices were incubated in RPMI 1640 medium containing 10% FBS, 1% penicillin/streptomycin, and 0.5% Fungizone for an hour in 37°C in a humidified chamber with 5% CO_2. Lung slices were transferred to a 24-well cell culture plate and treated for 16–24 h in 37°C humidified chamber with 5% CO_2.

Statistical Analysis

Means $\pm$ SD were calculated, and statistically significant differences between two groups were determined using the Student's *t* test. For three or more groups, statistical analysis was performed using one-way analysis of variance, followed by the Bonferroni's post analysis, as appropriate; $p < 0.05$ was considered statistically significant. For mRNA half-life, linear regression was calculated and confidence intervals were determined. Statistical software for all analysis was SigmaStat 3.1 (Systat Software, Point Richmond, CA).

RESULTS

HGF Inhibits Ang II-induced Intrinsic Apoptosis

HGF attenuates cellular apoptosis associated with fibrotic remodeling in the lung (Yaekashiwa *et al*., 1997; Dohi *et al*., 2000), but the mechanism of this activity is not completely understood. Previously, our laboratory reported that the profibrotic agent Ang II induces the intrinsic apoptotic pathway in primary ECs, with DNA fragmentation occurring within 24 h (Lee *et al*., 2010). We investigated the effect of HGF on Ang II-induced apoptosis in ECs by using the neutral comet assay, which detects chromosomal fragmentation as a function of apoptosis. Treatment with Ang II alone resulted in 65% apoptosis within 24 h. Pretreatment with HGF inhibited the Ang II-induced apoptosis, resulting in only 20% apoptosis ($p < 0.05$) (Figure 1A). To confirm that the cells are indeed undergoing apoptosis, we performed DNA laddering experiments. Data show that 25 ng/ml HGF pretreatment inhibited Ang II-induced DNA laddering (Figure 1B). HGF also prevented Ang II-induced caspase-3 activation and mitochondrial release of cytochrome *c*, as determined by western blot (Figure 1C).

HGF Inhibits Ang II Reduction of Bcl-x_L mRNA Half-Life

The down-regulation of anti-apoptotic members of the Bcl-2 family, relative to proapoptotic family members is sufficient to induce apoptosis. Our laboratory demonstrated that Ang II treatment of EC decreased levels of the anti-apoptotic protein Bcl-x_L and thereby reduced interaction of Bcl-x_L with the proapoptotic Bax protein (Lee *et al*., 2010). Pretreatment of EC with HGF before exposure to Ang II restored Bcl-x_L protein expression to basal levels (Figure 2A) and preserved its interaction with Bax (Figure 2B).

We demonstrated previously that Ang II decreases the half-life of Bcl-x_L mRNA (Lee *et al*., 2010). We therefore hypothesized that HGF would prevent Ang II-induced degradation of Bcl-x_L mRNA. The level of Bcl-x_L mRNA in the cells pretreated with HGF was stabilized in the presence of Ang II treatment (Figure 2C). These data suggest that one mechanism by which HGF prevents Ang II-induced decrease of Bcl-x_L protein levels is through stabilization of the Bcl-x_L mRNA.

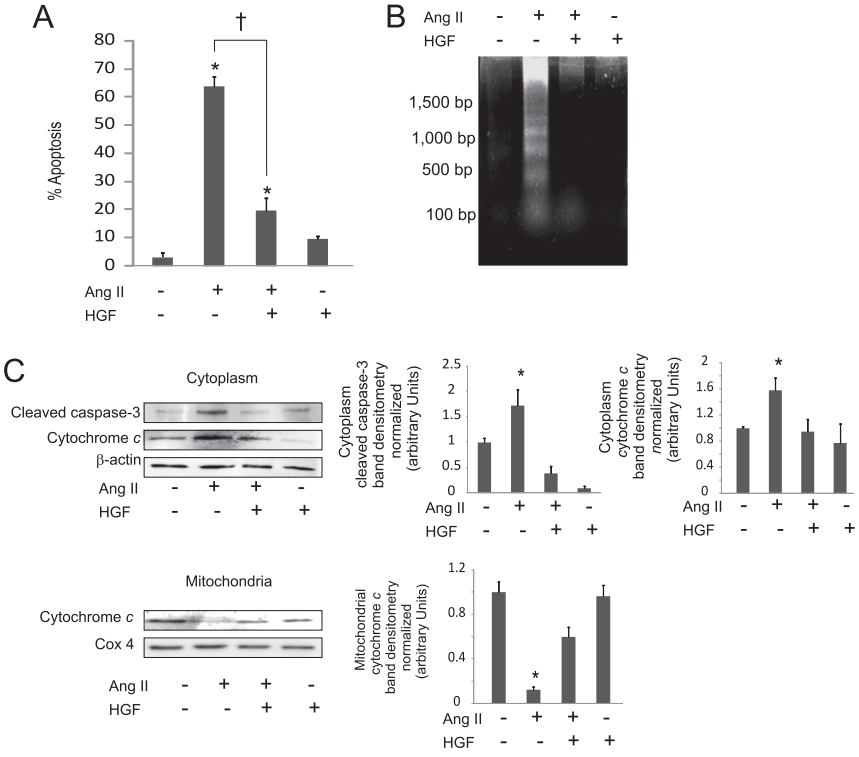

Figure 1. HGF inhibits Ang II-induced intrinsic apoptosis in ECs. ECs were grown to 80% confluence and starved in 0.01% FBS media overnight. Cells were treated with HGF (25 ng/ml) for 20 min before 10 μM Ang II for 24 h. (A) Neutral comet assay on HGF and Ang II-treated EC was done. The percentage of apoptotic cells are indicated. Data show means ± SD, n = 4. Asterisk (*) indicates statistical significance from control, $p < 0.05$. Dagger (†) indicates statistical significance from Ang II alone, $p < 0.05$. (B) Equal amounts of DNA were electrophoresed in agarose gels to visualize DNA laddering; representative data are shown. (C) Cells were lysed and mitochondria were removed from the cytosolic components. Cytosolic lysates were western blotted for cytochrome *c* and cleaved caspase-3. Right panels indicate densitometries, normalized to β-actin. Data show mean band density normalized to actin ± SD, n = 4. Asterisk (*) indicates statistical significance from control, $p < 0.05$. All experiments were repeated at least four times.

HGF-activated ERK1/2 Is Required for Inhibition of Ang II-induced Apoptosis

Binding of the Met receptor by HGF leads to the activation of two major antiapoptotic pathways, the ERK1/2 MAPK pathway and the PI3K pathway. We demonstrated that these pathways are both activated by HGF in ECs (Lee *et al.*, 2008). We investigated whether HGF uses the ERK1/2 or the PI3K pathway to inhibit Ang II-induced apoptosis. EC were

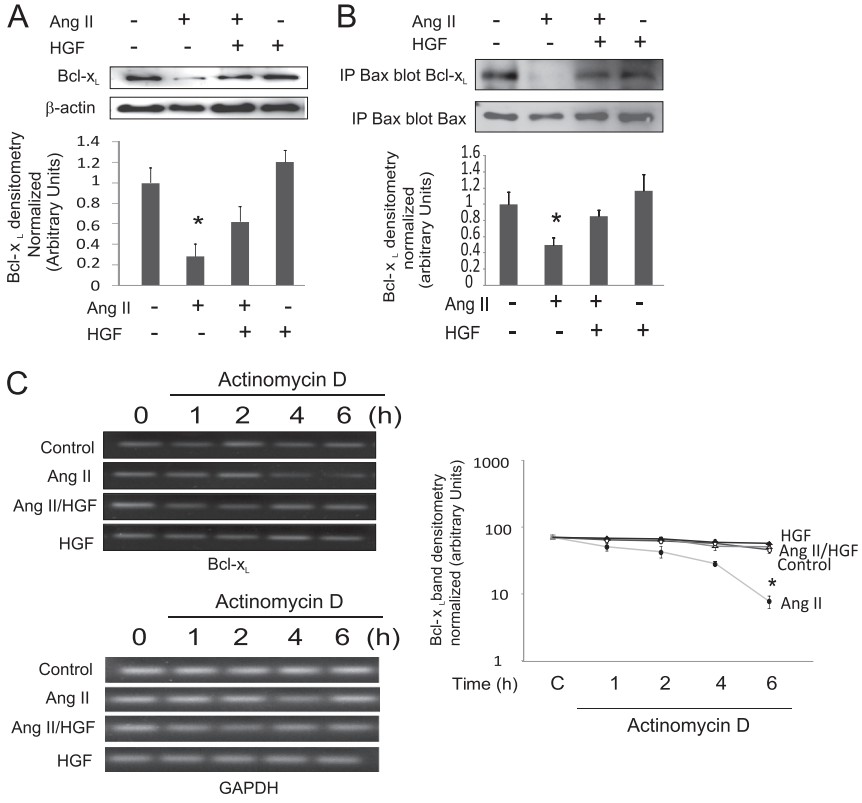

Figure 2. HGF inhibits Ang II-induced reduction of Bcl-x_L protein and mRNA. ECs were grown to 80% confluence and were placed in low serum (0.01% FBS) overnight. Cells were pretreated with HGF (25 ng/ml) for 20 min before treatment with 10 μM Ang II for 16 h. (A) Cell lysates were immunoblotted for Bcl-x_L protein expression; blots were stripped and reprobed for β-actin. Bottom panel shows densitometry of Bcl-x_L normalized to β-actin from three independent experiments. (B) Equal amounts of protein from cell lysates were immunoprecipitated for Bax and western blotted for Bcl-x_L. Blots were stripped and blotted for Bax. Bottom panel shows densitometry of Bcl-x_L normalized to Bax from three independent experiments. (C) Cells were pretreated with HGF (25 ng/ml) for 20 min before treatment with 10 μM Ang II for 8 h. After the treatment, 5 μg/ml actinomycin D was added. At various time points, total RNA was extracted, and the levels of Bcl-x_L mRNA were determined by RT-PCR. GAPDH was determined by RT-PCR as a control. For all graphs, data show means, ± SD, n = 3. Asterisk (*) indicates statistical significance from control, $p < 0.05$. At least three independent experiments were performed.

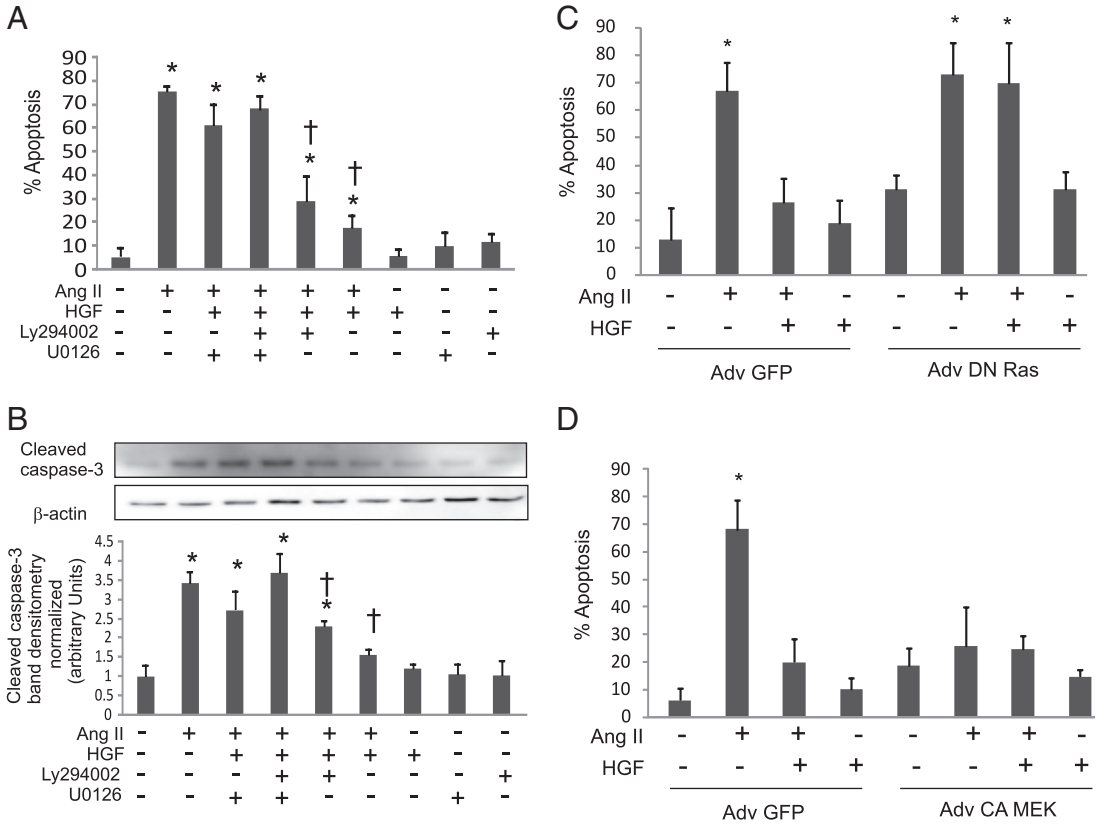

Figure 3. HGF-activated ERK1/2, but not PI3K, is necessary to inhibit apoptosis. (A and B) ECs were grown to 80% confluence and were placed in low serum (0.01% FBS) overnight. Cells were then pretreated with U0126 (10 μM), LY294002 (10 μM), HGF (25 ng/ml), or a combination for 20 min before treatment with 10 μM Ang II for 24 h. (A) Neutral comet assay. (B) Immunoblotting, using equal amounts of protein from whole cell lysates, was performed to determine the levels of cleaved caspase-3. Blots were stripped and blotted for β-actin to control for protein loading. (C and D) ECs were grown to 80% confluence and infected with adenovirus DN RAS or CA MEK for 48 h. Cells were then pretreated with HGF (25 ng/ml) for 20 min before treatment with 10 μM Ang II for 24 h. Neutral comet assay was performed. Data show means ± SD, n = 4. Asterisk (*) indicates statistical significance from control, $p < 0.05$. Dagger (†) indicates statistical significance from Ang II alone, $p < 0.05$. Experiments were repeated at least four times.

treated with Ang II and HGF with either the MEK1/2 inhibitor U0126 that blocks activation of ERK1/2 or LY294002 that inhibits PI3K activity. Ang II treatment alone induced ~75% apoptosis, and HGF pretreatment inhibited the cell death to ~20%, slightly above control levels (Figure 3A). U0126 treatment with HGF before the addition of Ang II eliminated HGF protection, and apoptosis was not statistically different from the addition of Ang II alone. LY294002 treatment had no significant effect on HGF inhibition of Ang II-induced apoptosis. When treated with both U0126 and LY294002 treatment before HGF and Ang II, the level of apoptosis was not significantly different from the level of apoptosis when U0126 was used alone. Addition of HGF, U0126, or LY294002 in the absence of Ang II did not induce significant apoptosis. Similar results were seen when using cleaved caspase-3 as a marker of apoptosis (Figure 3B). Ang II induced an ~3.5-fold increase in the band density of cleaved caspase-3 compared with control. HGF treatment reduced caspase-3 activation to basal levels. The inhibitory activity of HGF was significantly blocked by pretreatment with either U0126 or LY294002, although U0126 treatment demonstrated a greater inhibition of HGF activity. Addition of U0126 with LY294002 completely blocked HGF inhibition of Ang II-induced caspase-3 activation. The addition of HGF, U0126, or LY294002 in the absence of Ang II did not increase caspase activation above basal levels.

RAS and MEK1/2 are upstream signaling molecules of ERK1/2 pathway in Met signaling (Zhang and Vande Woude, 2003). Therefore, we used DN RAS to determine whether cell survival by HGF is also RAS dependent. DN RAS suppressed HGF-induced cell survival (Figure 3C). We next investigated the effect of overexpression of constitutively active (CA) MEK1 in ECs on Ang II-induced apoptosis. CA MEK1 overexpression provided complete inhibition of Ang II-induced apoptosis and did not affect the antiapoptotic activity of HGF (Figure 3D). Together these results suggest that HGF activation of Ras is required for its antiapoptotic activity, and activation of MEK1 alone is sufficient to inhibit Ang II-induced apoptosis.

HGF Protects the Interaction between Cytoplasmic Nucleolin and the 3′-UTR of the Bcl-x_L mRNA

Nucleolin protein binds to 3′-UTR of Bcl-x_L mRNA to stabilize the mRNA and prevent its degradation (Zhang *et al*., 2008a). Our laboratory showed that Ang II causes displacement of nucleolin from the Bcl-x_L mRNA in ECs, resulting in a decreased half-life of the mRNA (Lee *et al*., 2010). RNA-IP was performed to test whether HGF prevents Ang II-induced displacement of nucleolin from Bcl-x_L mRNA. Ang II

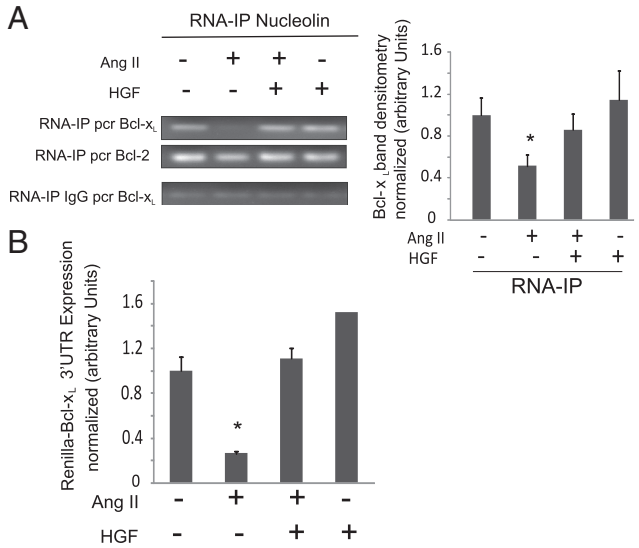

Figure 4. HGF stabilizes Bcl-x_L mRNA binding to nucleolin. ECs were grown to 80% confluence and were placed in low serum (0.01% FBS) overnight. Cells were then pretreated with HGF (25 ng/ml) for 20 min before treatment with 10 μM Ang II for 24 h. (A) Cells were fixed and RNA-IP was performed using the C23-nucleolin antibody. RNA–protein complex was reverse cross-linked for 2 h, and proteinase K and DNase were added. Phenol:chloroform RNA extraction was performed for cDNA synthesis. PCR was performed for the second AU-rich region of the 3′-UTR of Bcl-x_L. Bottom panel shows densitometry of Bcl-x_L mRNA band. Data show means ± SD, n = 3. Asterisk (*) indicates statistical significance from control, $p < 0.05$. (B) Cells were transfected with *Renilla*-Bcl-x_L 3′-UTR and cotransfected with a luciferase vector RSV-Luc construct to normalize for transfection efficiency. Six hours after transfection, cells were placed in serum-free medium. Cells were pretreated ± HGF (25 ng/ml) before treatment with 10 μM Ang II for 16 h. Luciferase and *Renilla* assays were performed on cell lysates. Data show means ± SD. Asterisk (*) indicates statistical significance from control, $p < 0.05$, n = 3. Experiments were repeated at least three times.

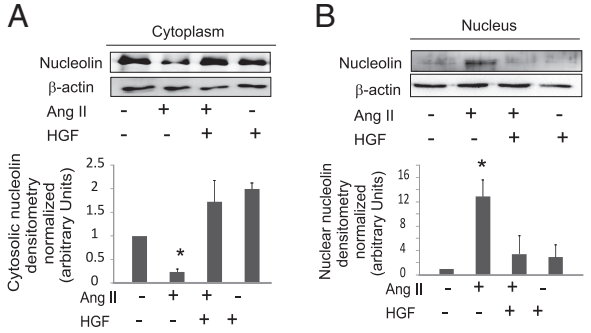

Figure 5. HGF blocks nucleolin translocation to the nucleus. ECs were grown to 80% confluence and were placed in low serum (0.01% FBS) overnight. Cells were then pre-treated with HGF (25 ng/ml) for 20 min before treatment with 10 μM Ang II for 24 h. After Ang II ± HGF treatment, cytosolic and nuclear fractions were used for nucleolin immunoblotting. Blots were stripped and blotted for β-actin to control for protein loading. Data show means ± SD, n = 3. Asterisk (*) indicates statistical significance from control, $p < 0.05$. Experiments were repeated at least three times.

decreased the level of Bcl-x_L mRNA bound to nucleolin by ~60% (Figure 4A). HGF pretreatment maintained the Bcl-x_L–nucleolin complex at basal levels. To confirm these findings, we tested the effects of HGF on a *Renilla* expression construct containing the Bcl-x_L 3′-UTR that is responsive to nucleolin stabilization (Zhang *et al.*, 2008a). Ang II decreased the levels of *Renilla*-Bcl-x_L by ~75% (Figure 4B). In contrast, HGF pretreatment inhibited the Ang II-induced decrease, restoring the levels of *Renilla* to basal levels. These data indicate that HGF prevents Ang II-induced disassociation between nucleolin and Bcl-x_L mRNA.

HGF Blocks Ang II-induced Translocation of Nucleolin to the Nucleus

In apoptotic cells, nucleolin has been observed to undergo nuclear translocation as well as proteolytic processing (Srivastava and Pollard, 1999; Kito *et al.*, 2003). We hypothesized that Ang II-induced nuclear translocation, degradation, or both of nucleolin might contribute to the decreased availability of nucleolin for binding to the Bcl-x_L mRNA; we further hypothesized that HGF might prevent the degradation or nuclear localization of nucleolin. Nuclear and cytoplasmic fractions were examined for nucleolin protein by using western blot analysis after Ang II treatment, HGF treatment, or both of ECs. Ang II decreased the cytoplasmic levels of nucleolin protein by ~70% and significantly increased nucleolin levels in the nucleus compared with control (Figure 5). Although other researchers have reported that nucleolin may undergo proteolysis during apoptosis, we did not detect lower-molecular-weight bands under our experimental conditions (data not shown). HGF inhibited the Ang II-induced translocation of nucleolin from the cytoplasm to the nucleus, maintaining nucleolin in the cytoplasm to near basal levels. These data indicate that Ang II reduces the level of nucleolin in the cytoplasm via nuclear translocation and that HGF inhibits this relocalization.

HGF Stabilization of the Binding of Nucleolin to the Bcl-x_L 3′-UTR Requires ERK1/2 Pathway

Prior studies of HGF-induced cell survival suggested the involvement of two major pathways for this activity: the ERK1/2 and PI3K/Akt pathways (Day *et al.*, 1999; Fan *et al.*, 2000). To determine which pathway HGF uses for stabilization of the nucleolin–Bcl-x_L mRNA complex, cells were treated with either the MEK1/2 inhibitor U0126 or PI3K inhibitor LY294002 before the addition HGF and Ang II. Pretreatment with U0126 blocked the effect of HGF on Ang II-induced localization of nucleolin to the nucleus (Figure 6, A and B). However, LY294002 treatment did not affect HGF inhibition of Ang II-induced nucleolin translocation. We next examined the effect of inhibiting the ERK1/2 pathway on the Bcl-x_L mRNA levels. In agreement with our previous findings, quantitative RT-PCR showed that the MEK1/2 inhibitor U0126 blocked HGF inhibition of Ang II-induced down-regulation Bcl-x_L mRNA (Figure 6C). Again, LY294002 treatment did not alter the level of the Bcl-x_L mRNA induced by HGF treatment (Figure 6C). Using the *Renilla* expression construct containing the Bcl-x_L 3′-UTR, we observed that HGF inhibited Ang II-induced decrease of *Renilla* expression (Figure 6D). Interestingly, levels of *Renilla*-Bcl-x_L 3′-UTR levels were increased by HGF treatment alone to ~20% over control levels. ERK1/2 inhibition prevented HGF inhibition of Ang II destabilization of the *Renilla* reporter (Figure 6D). We found that LY294002 does not prevent HGF inhibition of Ang II destabilization of the *Renilla* reporter (data not shown).

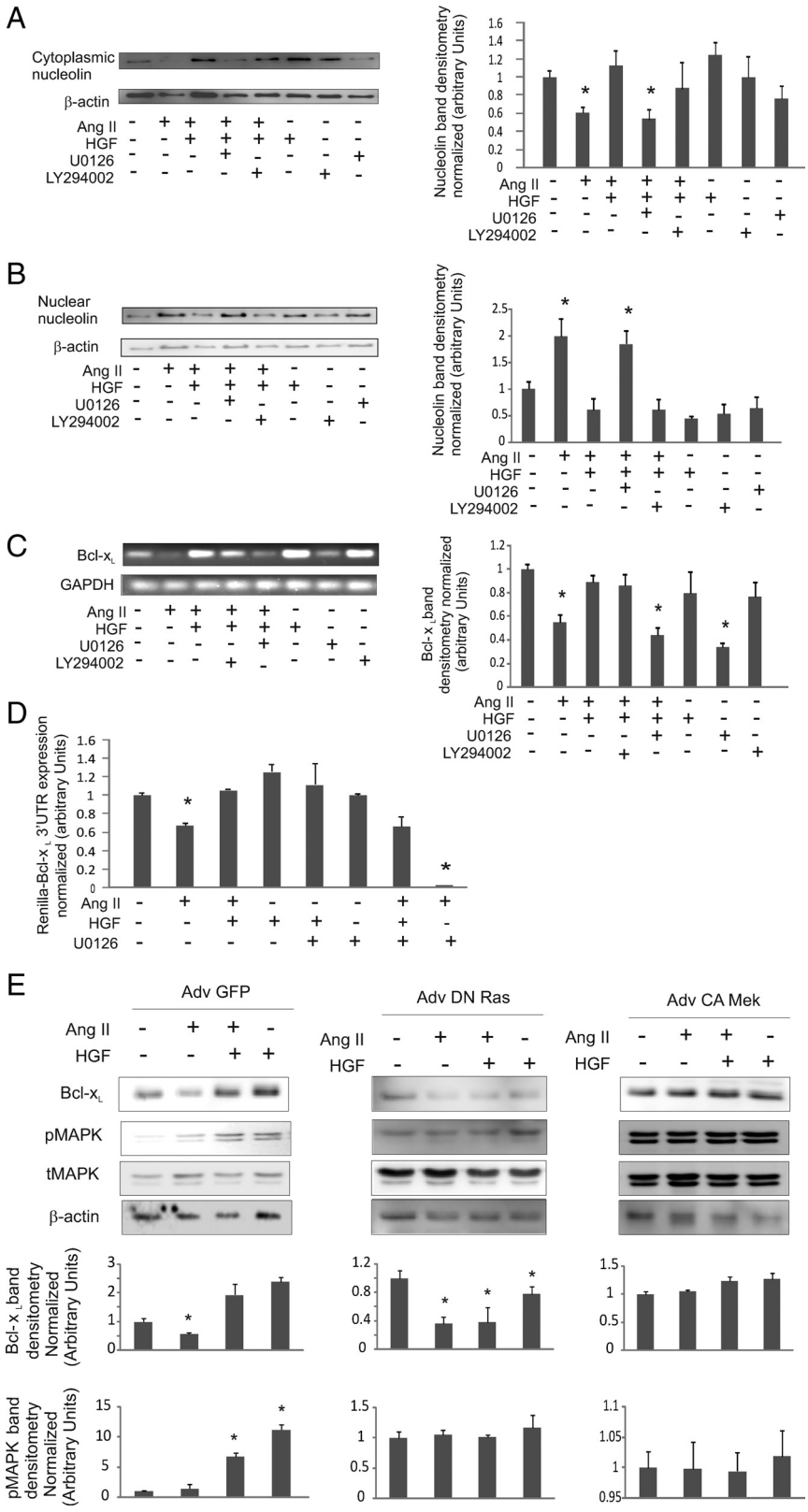

Figure 6. The ERK1/2 pathway is required for HGF localization of nucleolin to the cytoplasm. (A–C) ECs were grown to 80% confluence and were placed in low serum (0.01% FBS) overnight. Cells were then pretreated with HGF (25 ng/ml) for 20 min ± either LY294002 (10 μM) or U0126 (10 μM) for 20 min, before the addition of 10 μM Ang II for 24 h. (A) Cytosolic extracts were analyzed for the nucleolin protein by using western blotting. (B) Nuclear extracts were analyzed for the nucleolin protein by using immunoblotting. Blots were stripped and blotted for β-actin to control for protein loading. All data show means ± SD, n = 3. Asterisk (*) indicates statistical significance from control, $p < 0.05$. Experiments were repeated at least three times. (C) RNA-IP was performed for nucleolin followed by PCR amplification for the second AU-rich region of the 3′-UTR of Bcl-x_L. (D) ECs were transfected with *Renilla*-Bcl-x_L 3′-UTR and cotransfected with a luciferase vector RSV-Luc construct to normalize for transfection efficiency. Six hours after transfection, cells were placed in serum-free medium. Cells were pretreated ± U0126 (10 μM) before treatment with HGF (25 ng/ml) for 16 h. Luciferase and *Renilla* assays were performed on cell lysates. Data show means ± SD. Asterisk (*) indicates statistical significance from control, $p < 0.05$, n = 4. Experiments were repeated at least four times. (E) ECs were grown to 80% confluence and infected with adenovirus for 48 h. Cells were then pretreated with HGF (25 ng/ml) for 20 min before treatment with 10 μM Ang II for 24 h. Immunoblotting, using equal amounts of protein from whole cell lysates, was performed to determine the levels of Bcl-x_L and phospho-MAPK (pMAPK). Blots were stripped and blotted for total MAPK (tMAPK) and β-actin to control for protein loading. Data show means ± SD, n = 3. Asterisk (*) indicates statistical significance from control, $p < 0.05$. Dagger (†) indicates statistical significance from Ang II alone, $p < 0.05$. Experiments were repeated at least three times.

To confirm the role of the Ras/MEK1/2/ERK1/2 pathway, EC were infected with adenovirus DN Ras or CA MEK1. When the cells were infected with DN Ras, the level of Bcl-x_L decreased significantly even with the HGF treatment (Figure 6E). In addition, dominant-negative RAS inhibited HGF-induced ERK activation, showing that ERK activation by HGF is downstream of RAS activation (Figure 6E). In contrast, constitutively active MEK1 ex-

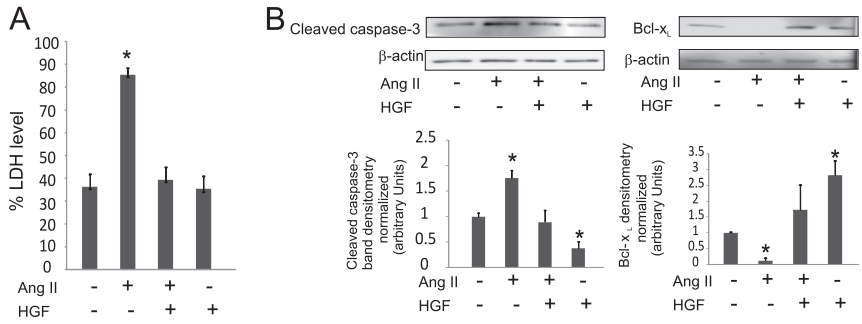

Figure 7. HGF inhibits Ang II-induced apoptosis in rat lung ex vivo cultures. (A and B) Rat lung slices were cultured overnight in a media containing 10 μM Ang II ± HGF (25 ng/ml) for 24 h. (A) Cell media were collected to quantify the LDH release. (B) Lung slice tissue was homogenized and the protein lysates were used for western blots to determine the levels of Bcl-x_L and activated caspase-3. Data show means ± SD. Asterisk (*) indicates statistical significance from control, $p < 0.05$, $n = 4$. Experiments were repeated at least four times.

pression in EC alone protected Bcl-x_L levels (Figure 6E). Together, these data suggest that HGF-activated ERK1/2, but not PI3K, is required for HGF-induced cytoplasmic localization of nucleolin and stabilization of Bcl-x_L mRNA.

HGF Inhibits Ang II-induced Apoptosis in Ex Vivo Rat Lung Tissue

Ex vivo lung slice cultures have been used as an alternative to in vivo experiments for measuring cellular signaling mechanisms. In the ex vivo method, an isolated organ sustains the architecture and functionality of the tissue, thus represents a closer model to in vivo than the in vitro monolayer models from a single cell type. Studies have shown that alveolar cells divide and correctly differentiate in ex vivo lung slice cultures (Kinnard *et al*., 1994), and this technique has been used for apoptosis and cell survival studies (Li *et al*., 2003; Lang *et al*., 2007; Hackett *et al*., 2008). The ex vivo lung model has been demonstrated to act as a reliable model for in vivo studies of the role of Ang II signaling inducing lung cell apoptosis downstream of profibrotic stimuli (Li *et al*., 2003; Mancini and Khalil, 2005). We therefore used lung explants with Ang II treatment with or without HGF to verify our EC monoculture findings. A lactate dehydrogenase (LDH)-cytotoxicity assay was performed to evaluate cell death. Ang II treatment induced an ~2.4-fold increase in LDH levels compared with the untreated control (Figure 7A). Cotreatment of Ang II with HGF reduced LDH to basal levels.

Ang II activated proapoptotic proteins in the lung slice explants, consistent with our findings in EC cultures (Figure 7B). The data demonstrate that HGF inhibited cleaved caspase-3 induced by Ang II treatment. Ang II treatment also lowered the level of Bcl-x_L protein level, but with HGF, the level of Bcl-x_L protein was similar to the control (Figure 7B). Interestingly, treatment of the lung explants with HGF alone reduced levels of caspase-3 and increased levels of Bcl-x_L protein compared with basal levels. This suggests that HGF prevents cell death that might occur from the processing of the tissue for slice cultures.

HGF Activated ERK1/2 Inhibits Ang II-induced Apoptosis in Ex Vivo Rat Lung Slices

To confirm that HGF activation of ERK1/2 is necessary to inhibit Ang II-induced apoptosis in explant tissue, we first used chemical MEK1/2 inhibitor U0126. Ang II treatment of ex vivo rat lung explants increased levels of cleaved caspase-3, but pretreatment with HGF prevented cleavage of caspase-3 (Figure 8A, top). When the lung slices were pretreated with U0126 before HGF and Ang II treatments, the level of active caspase-3 increased. To verify that U0126 can enter and inhibit MEK in the tissue, a control experiment was performed, showing that phosphorylated ERK1/2 is present in the tissue and can be inhibited by U0126 (Figure 8A, bottom). Next, we used overexpression of DN MEK1 to verify our findings using pharmacological inhibition of MEK to block ERK1/2 activation. Lung explant tissues were infected with either adenovirus-encoded green fluorescent protein (GFP), as a control, or adenovirus-encoded DN MEK1. Adenovirus-GFP was used to confirm viral incorporation and gene expression in the lung ex vivo explants (data not shown). After infection, lung explants were treated with HGF and Ang II. Overexpression of GFP did not affect HGF activation of ERK1/2, but overexpression of DN MEK1 blocked this activation (Figure 8B, left). Adenovirus-GFP tissues treated with Ang II contained increased active caspase-3, but HGF treatment significantly reduced cleaved caspase-3 levels (Figure 8B, right). Adenovirus-DN MEK1-infected tissue showed increased levels of caspase-3 activation in the presence of Ang II as well as HGF (Figure 8B, right). Together, the data suggest that HGF uses the ERK1/2 pathway to inhibit apoptosis in lung explant tissue.

DISCUSSION

HGF has been demonstrated to function as an antifibrotic factor, but the mechanism of this activity is not completely understood. Here, we demonstrate that HGF inhibits the apoptotic activity of Ang II, a key factor in the progression of fibrotic organ diseases (Filippatos *et al*., 2001; Marshall *et al*., 2004; Konigshoff *et al*., 2007; Wynn, 2008). We found previously that Ang II induces the intrinsic mechanism of apoptosis in EC through the reduction of Bcl-x_L protein and mRNA levels (Lee *et al*., 2010). In our current work, we demonstrate using both in vitro and ex vivo models that HGF inhibits Ang II-induced apoptosis, blocking cytochrome *c* release from the mitochondria, caspase-3 activation, and DNA fragmentation. This blockade involves the stabilization of anti-apoptotic Bcl-x_L mRNA via the binding of nucleolin. Our data indicate that HGF inhibition of Ang II-induced apoptosis, including stabilization of Bcl-x_L mRNA, is dependent upon the activation of ERK1/2.

In cancer cells, the mechanism of HGF-induced cell growth and inhibition of apoptosis has been shown to involve two major pathways, ERK1/2 and PI3K (Day *et al*., 1999; Fan *et al*., 2000; Xiao *et al*., 2001). Others have shown that HGF can inhibit the intrinsic apoptotic pathway by dual mechanisms, involving phosphorylation and deactivation of proapoptotic Bcl-2 family members as well as the up-regulation of antiapoptotic Bcl-2 family members (del Peso *et al*., 1997; Zhang *et al*., 2008b). PI3K has shown to increase Bcl-x_L gene expression to prevent apoptosis in some cell types (Umeda *et al*., 2003). In addition, previous studies have shown that Akt, a kinase activated downstream of PI3K, exerts antiapoptotic effects through the phosphorylation of

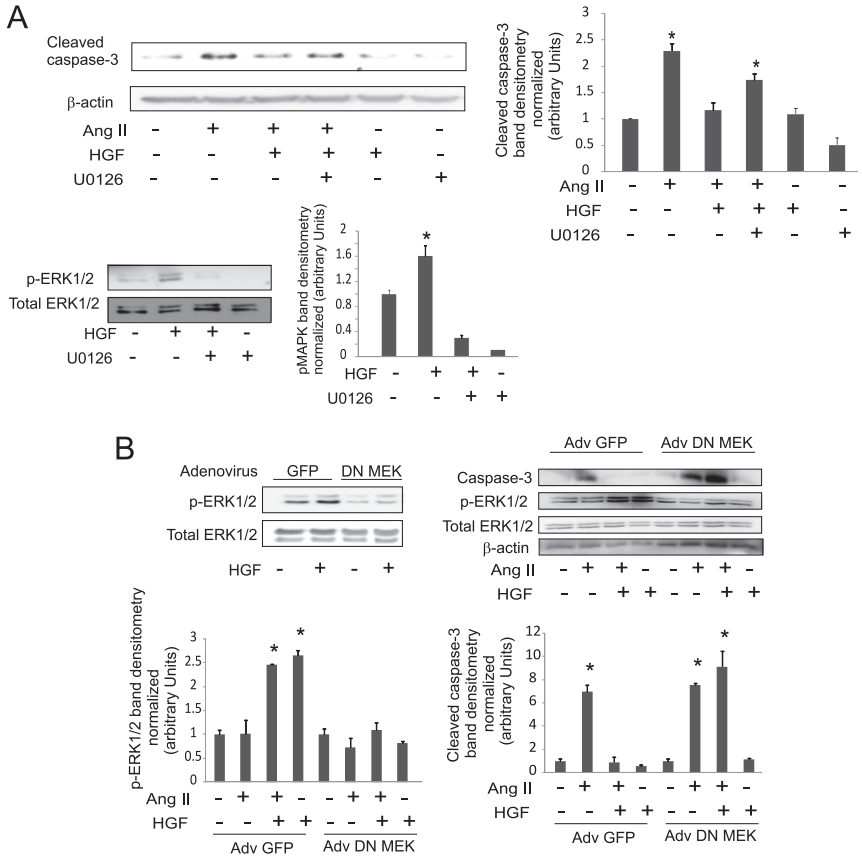

Figure 8. HGF-activated ERK1/2 is necessary to inhibit apoptosis in rat lung ex vivo explants. (A) Ex vivo rat lung slices were treated with Ang II (10 μM) ± U0126 (10 μM) and/or HGF (25 ng/ml) overnight. The tissue was homogenized, and the protein lysates were used for Western blots to determine the expression level of cleaved caspase-3. ERK1/2 phosphorylation by HGF was determined after 10 min of treatment with HGF (25 ng/ml) ± U0126 (10 μM). Equal amounts of protein lysates were immunoblotted for phospho-ERK1/2 (p-ERK1/2); blots were stripped and blotted for total ERK1/2 as a control. Panel to the right shows densitometry of p-ERK1/2 normalized to total ERK1/2. (B) Rat lung tissue slice cultures were infected with adenovirus GFP or DN MEK for 48 h, followed by treatment overnight with Ang II (10 μM) ± HGF (25 ng/ml). Tissues were homogenized, and whole cell lysates were used to run western blots for p-ERK1/2 and cleaved caspase-3; blots were stripped and probed for total ERK1/2 and β-actin, respectively, for protein loading controls. For all bar graphs, data show means ± SD. Asterisk (*) indicates statistical significance from control, $p < 0.05$, $n = 3$. Experiments were repeated at least three times.

nucleolin (Barel *et al*., 2003; Borgatti *et al*., 2003). Previous reports indicate that ERK1/2 also increases cell survival by several mechanisms, including via the regulation of the phosphorylation state of antiapoptotic proteins (Horiuchi *et al*., 1997; Ito *et al*., 1997). Both PI3K and ERK1/2 pathways are activated by HGF to decrease caspase-3 activation after serum starvation or UV irradiation, although it is not known whether these effects are direct or indirect (Xiao *et al*., 2001).

Our current findings indicate that ERK1/2 inhibition, but not PI3K inhibition, blocks HGF survival activity in the presence of Ang II. Our data indicate that activation of the ERK1/2 pathway is both necessary and sufficient to inhibit Ang II-induced apoptosis. Results from cell culture experiments using the overexpression of CA MEK1 demonstrate that CA MEK1 alone prevents degradation of antiapoptotic Bcl-x_L protein and inhibits Ang II-induced apoptosis. Overexpression of DN Ras, upstream of ERK1/2 activation, blocks HGF inhibition of Ang II-induced apoptosis. These findings further suggest that other growth factors that sufficiently activate the MEK/ERK pathway will also inhibit Ang II-induced translocation of nucleolin to the nucleus and its disassociation from the Bcl-x_L mRNA with subsequent down-regulation of Bcl-x_L protein and apoptosis.

Our data also indicate that HGF promotes the binding of the protein nucleolin to the Bcl-x_L mRNA to prevent Ang II-induced reduction of this mRNA. The multifunctional protein nucleolin binds to RNA and DNA and plays roles in proliferation, apoptosis, and differentiation (Sengupta *et al*., 2004). In the cytoplasm, nucleolin protects Bcl-2 and Bcl-x_L mRNAs from degradation by binding to AU-rich regions of the 3′-UTRs, thus contributing to cell survival by stabilizing the levels of these anti-apoptotic members of the Bcl-2 family (Sengupta *et al*., 2004; Otake *et al*., 2007). Previously, we found that Ang II caused a decrease in Bcl-x_L mRNA half-life by reducing the nucleolin binding to the second AU-rich region of the UTR of the mRNA (Lee *et al*., 2010). We demonstrated that although nucleolin binds to both Bcl-x_L and Bcl-2 mRNA in EC, Ang II treatment specifically reduces nucleolin binding to Bcl-x_L but not to Bcl-2 (Lee *et al*., 2010). This was reflected in the reduction of Bcl-x_L protein but not of Bcl-2 protein, suggesting Bcl-2 protein does not play a major role in Ang II-induced apoptosis.

Several studies have indicated that nucleolin protein might play a pivotal role in the balance between cell survival and apoptosis. Down-regulation of nucleolin, by small interfering RNA or by agents that cause its degradation, is sufficient to induce growth arrest and apoptosis (Kito *et al*., 2003; Ugrinova *et al*., 2007). Nucleolin can be regulated through proteolysis, methylation, ADP-ribosylation, and phosphorylation (Srivastava and Pollard, 1999). Specific phosphorylations affect nucleolin's stability and subcellular localization (Schwab and Dreyer, 1997). In the cytoplasm, nucleolin plays a role in cell survival but its translocation to the nucleus is associated with proapoptotic events (Schwab and Dreyer, 1997). In the cytoplasm, nucleolin can be phosphorylated by protein kinase C (PKC), cyclic AMP-dependent protein kinase (PKA), and ectoprotein kinase (Srivastava and Pollard, 1999). Nucleolin contains its own nuclear translocation signal, but nuclear translocation of nucleolin requires dephosphorylation (Schwab and Dreyer, 1997). In the nucleus, nucleolin can be phosphorylated on serine residues by the cell cycle-regulated kinases casein kinase II and cell division cycle 2 protein, resulting in its localization back to the cytoplasm (Peter *et al*., 1990; Bouche *et al*., 1994). We recently determined that Ang II-induced nuclear translocation of nucleolin and its dissociation from Bcl-x_L mRNA

requires the activation of the protein phosphatase SHP-2 (Lee *et al*., 2010). We also determined that neither PKC nor PKA affected apoptosis by Ang II (Lee *et al*., 2010), suggesting that these two kinases are not involved in this pathway. The exact mechanism of the effect of ERK activation on nucleolin is not known. This issue is currently under investigation in our laboratory.

Our work also demonstrates that HGF inhibits Ang II-induced apoptosis in lung tissue ex vivo. Studies using the ex vivo method have indicated that alveolar cells divide and correctly differentiate in ex vivo lung slice cultures (Kinnard *et al*., 1994), and this technique has been used for apoptosis and cell survival studies (Li *et al*., 2003; Lang *et al*., 2007; Hackett *et al*., 2008). The in vivo mechanism(s) of HGF-induced cell survival is currently being investigated in our laboratory. The identification of key downstream signaling for the inhibition of cellular apoptosis during the progression of fibrosis may lead to the development of novel drug targets for this disease.

ACKNOWLEDGMENTS

We thank Dr. Suzanne B. Bausch and W. Bradley Rittase (Uniformed Services University of the Health Sciences) for rat lung tissue and help in development of the ex vivo lung culture technique. We also thank Dr. G. Timothy Bowden for providing the *Renilla*-Bcl-x_L construct, Dr. Mary Lou Cutler for providing DN Ras adenovirus, and Dr. Yuichiro J. Suzuki for providing the dominant-negative-MEK and constitutive active-MEK adenovirus. This work was supported by National Institutes of Health grant HL-073929 and a Uniformed Services University of the Health Sciences research grant (to R.M.D.) and by a predoctoral fellowship from the American Heart Association (to Y.H.L.). Some of the authors are employees of the U.S. Government. This work was prepared as part of their official duties. Title 17 U.S.C. §105 provides that 'Copyright protection under this title is not available for any work of the United States Government.' Title 17 U.S.C. §101 defined a U.S. Government work as a work prepared by a military service member or employees of the U.S. Government as part of that person's official duties. The views in this article are those of the authors and do not necessarily reflect the views, official policy, or position of the Uniformed Services University of the Health Sciences, Department of the Navy, Department of Defense, or the U.S. Federal Government.

REFERENCES

Barel, M., Balbo, M., Le Romancer, M., and Frade, R. (2003). Activation of Epstein-Barr virus/C3d receptor (gp140, CR2, CD21) on human cell surface triggers pp60src and Akt-GSK3 activities upstream and downstream to PI 3-kinase, respectively. Eur. J. Immunol. *33*, 2557–2566.

Borgatti, P., Martelli, A. M., Tabellini, G., Bellacosa, A., Capitani, S., and Neri, L. M. (2003). Threonine 308 phosphorylated form of Akt translocates to the nucleus of PC12 cells under nerve growth factor stimulation and associates with the nuclear matrix protein nucleolin. J. Cell Physiol. *196*, 79–88.

Bouche, G., Baldin, V., Belenguer, P., Prats, H., and Amalric, F. (1994). Activation of rDNA transcription by FGF-2, key role of protein kinase CKII. Cell. Mol. Biol. Res. *40*, 547–554.

Brunet, A., Bonni, A., Zigmond, M. J., Lin, M. Z., Juo, P., Hu, L. S., Anderson, M. J., Arden, K. C., Blenis, J., and Greenberg, M. E. (1999). Akt promotes cell survival by phosphorylating and inhibiting a Forkhead transcription factor. Cell *96*, 857–868.

Day, R. M., Cioce, V., Breckenridge, D., Castagnino, P., and Bottaro, D. P. (1999). Differential signaling by alternative HGF isoforms through c-Met: activation of both MAP kinase and PI 3-kinase pathways is insufficient for mitogenesis. Oncogene *18*, 3399–3406.

del Peso, L., Gonzalez-Garcia, M., Page, C., Herrera, R., and Nunez, G. (1997). Interleukin-3-induced phosphorylation of BAD through the protein kinase Akt. Science *278*, 687–689.

Dohi, M., Hasegawa, T., Yamamoto, K., and Marshall, B. C. (2000). Hepatocyte growth factor attenuates collagen accumulation in a murine model of pulmonary fibrosis. Am. J. Respir. Crit. Care Med. *162*, 2302–2307.

Ebina, M., Shimizukawa, M., Narumi, K., Miki, M., Koinuma, D., Watabe, M., Munakata, H., and Nukiwa, T. (2002). Towards an effective gene therapy for idiopathic pulmonary fibrosis. Chest *121*, 32S–33S.

Fan, S., Ma, Y. X., Wang, J. A., Yuan, R. Q., Meng, Q., Cao, Y., Laterra, J. J., Goldberg, I. D., and Rosen, E. M. (2000). The cytokine hepatocyte growth factor/scatter factor inhibits apoptosis and enhances DNA repair by a common mechanism involving signaling through phosphatidyl inositol 3′ kinase. Oncogene *19*, 2212–2223.

Filippatos, G. S., Gangopadhyay, N., Lalude, O., Parameswaran, N., Said, S. I., Spielman, W., and Uhal, B. D. (2001). Regulation of apoptosis by vasoactive peptides. Am. J. Physiol. Lung Cell Mol. Physiol. *281*, L749–L761.

Hackett, T. L., Holloway, R., Holgate, S. T., and Warner, J. A. (2008). Dynamics of pro-inflammatory and anti-inflammatory cytokine release during acute inflammation in chronic obstructive pulmonary disease: an ex vivo study. Respir. Res. *9*, 47.

Horiuchi, M., Hayashida, W., Kambe, T., Yamada, T., and Dzau, V. J. (1997). Angiotensin type 2 receptor dephosphorylates Bcl-2 by activating mitogen-activated protein kinase phosphatase-1 and induces apoptosis. J. Biol. Chem. *272*, 19022–19026.

Ito, T., Deng, X., Carr, B., and May, W. S. (1997). Bcl-2 phosphorylation required for anti-apoptosis function. J. Biol. Chem. *272*, 11671–11673.

Kawaida, K., Matsumoto, K., Shimazu, H., and Nakamura, T. (1994). Hepatocyte growth factor prevents acute renal failure and accelerates renal regeneration in mice. Proc. Natl. Acad. Sci. USA *91*, 4357–4361.

Kinnard, W. V., Tuder, R., Papst, P., and Fisher, J. H. (1994). Regulation of alveolar type II cell differentiation and proliferation in adult rat lung explants. Am. J. Respir. Cell. Mol. Biol. *11*, 416–425.

Kito, S., Shimizu, K., Okamura, H., Yoshida, K., Morimoto, H., Fujita, M., Morimoto, Y., Ohba, T., and Haneji, T. (2003). Cleavage of nucleolin and argyrophilic nucleolar organizer region associated proteins in apoptosis-induced cells. Biochem. Biophys. Res. Commun. *300*, 950–956.

Kitta, K., Day, R. M., Ikeda, T., and Suzuki, Y. J. (2001). Hepatocyte growth factor protects cardiac myocytes against oxidative stress-induced apoptosis. Free Radic. Biol. Med. *31*, 902–910.

Konigshoff, M., Wilhelm, A., Jahn, A., Sedding, D., Amarie, O. V., Eul, B., Seeger, W., Fink, L., Gunther, A., Eickelberg, O., and Rose, F. (2007). The angiotensin II receptor 2 is expressed and mediates angiotensin II signaling in lung fibrosis. Am. J. Respir. Cell. Mol. Biol. *37*, 640–650.

Kosai, K., Matsumoto, K., Funakoshi, H., and Nakamura, T. (1999). Hepatocyte growth factor prevents endotoxin-induced lethal hepatic failure in mice. Hepatology *30*, 151–159.

Krown, K. A., Page, M. T., Nguyen, C., Zechner, D., Gutierrez, V., Comstock, K. L., Glembotski, C. G., Quintana, P.J.E., and Sabbadini, R. A. (1996). Tumor necrosis factor alpha-induced apoptosis in cardiac myocytes: involvement of the sphingolipid signaling cascade in cardiac cell death. J. Clin Invest. *98*, 2854–2865.

Lang, D. S., Droemann, D., Schultz, H., Branscheid, D., Martin, C., Ressmeyer, A. R., Zabel, P., Vollmer, E., and Goldmann, T. (2007). A novel human ex vivo model for the analysis of molecular events during lung cancer chemotherapy. Respir. Res. *8*, 43

Lee, Y. H., Mungunsukh, O., Tutino, R. L., Marquez, A. P., and Day, R. M. (2010). Angiotensin-II-induced apoptosis requires regulation of nucleolin and Bcl-x_L by SHP-2 in primary lung endothelial cells. J. Cell Sci. *123*, 1634–1643.

Lee, Y. H., Suzuki, Y. J., Griffin, A. J., and Day, R. M. (2008). Hepatocyte growth factor regulates cyclooxygenase-2 expression via beta-catenin, Akt, and p42/p44 MAPK in human bronchial epithelial cells. Am. J. Physiol. Lung Cell Mol. Physiol. *294*, L778–L786.

Li, X., Rayford, H., and Uhal, B. D. (2003). Essential roles for angiotensin receptor AT1a in bleomycin-induced apoptosis and lung fibrosis in mice. Am. J. Pathol. *163*, 2523–2530.

Mancini, G. B., and Khalil, N. (2005). Angiotensin II type 1 receptor blocker inhibits pulmonary injury. Clin. Invest. Med. *28*, 118–126.

Marshall, R. P., Gohlke, P., Chambers, R. C., Howell, D. C., Bottoms, S. E., Unger, T., McAnulty, R. J., and Laurent, G. J. (2004). Angiotensin II and the fibroproliferative response to acute lung injury. Am. J. Physiol. Lung Cell Mol. Physiol. *286*, L156–L164.

Matsumoto, K., and Nakamura, T. (1993). Roles of HGF as a pleiotropic factor in organ regeneration. EXS *65*, 225–249.

Matsumoto, K., and Nakamura, T. (2001). Hepatocyte growth factor: renotropic role and potential therapeutics for renal diseases. Kidney Int. *59*, 2023–2038.

Otake, Y., Soundararajan, S., Sengupta, T. K., Kio, E. A., Smith, J. C., Pineda-Roman, M., Stuart, R. K., Spicer, E. K., and Fernandes, D. J. (2007). Overexpression of nucleolin in chronic lymphocytic leukemia cells induces stabilization of bcl2 mRNA. Blood *109*, 3069–3075.

Peter, M., Nakagawa, J., Doree, M., Labbe, J. C., and Nigg, E. A. (1990). Identification of major nucleolar proteins as candidate mitotic substrates of cdc2 kinase. Cell *60*, 791–801.

Ponzetto, C., Bardelli, A., Zhen, Z., Maina, F., dalla Zonca, P., Giordano, S., Graziani, A., Panayotou, G., and Comoglio, P. M. (1994). A multifunctional docking site mediates signaling and transformation by the hepatocyte growth factor/scatter factor receptor family. Cell *77*, 261–271.

Rubin, J. S., Bottaro, D. P., and Aaronson, S. A. (1993). Hepatocyte growth factor/scatter factor and its receptor, the c-met proto-oncogene product. Biochim. Biophys. Acta *1155*, 357–371.

Schwab, M. S., and Dreyer, C. (1997). Protein phosphorylation sites regulate the function of the bipartite NLS of nucleolin. Eur. J. Cell Biol. *73*, 287–297.

Sengupta, T. K., Bandyopadhyay, S., Fernandes, D. J., and Spicer, E. K. (2004). Identification of nucleolin as an AU-rich element binding protein involved in bcl-2 mRNA stabilization. J. Biol. Chem. *279*, 10855–10863.

Srivastava, M., and Pollard, H. B. (1999). Molecular dissection of nucleolin's role in growth and cell proliferation: new insights. FASEB J. *13*, 1911–1922.

Ugrinova, I., Monier, K., Ivaldi, C., Thiry, M., Storck, S., Mongelard, F., and Bouvet, P. (2007). Inactivation of nucleolin leads to nucleolar disruption, cell cycle arrest and defects in centrosome duplication. BMC Mol. Biol. *8*, 66

Umeda, J., Sano, S., Kogawa, K., Motoyama, N., Yoshikawa, K., Itami, S., Kondoh, G., Watanabe, T., and Takeda, J. (2003). In vivo cooperation between Bcl-x_L and the phosphoinositide 3-kinase-Akt signaling pathway for the protection of epidermal keratinocytes from apoptosis. FASEB J. *17*, 610–620.

Wang, R., Ibarra-Sunga, O., Verlinski, L., Pick, R., and Uhal, B. D. (2000). Abrogation of bleomycin-induced epithelial apoptosis and lung fibrosis by captopril or by a caspase inhibitor. Am. J. Physiol. Lung Cell Mol. Physiol. *279*, L143–L151.

Wang, R., Ramos, C., Joshi, I., Zagariya, A., Pardo, A., Selman, M., and Uhal, B. D. (1999a). Human lung myofibroblast-derived inducers of alveolar epithelial apoptosis identified as angiotensin peptides. Am. J. Physiol. Lung Cell Mol. Physiol. *277*, L1158–L1164.

Wang, R., Zagariya, A., Ibarra-Sunga, O., Gidea, C., Ang, E., Deshmukh, S., Chaudhary, G., Baraboutis, J., Filippatos, G., and Uhal, B. D. (1999b). Angiotensin II induces apoptosis in human and rat alveolar epithelial cells. Am. J. Physiol. Lung Cell Mol. Physiol. *276*, L885–L889.

Watanabe, M., *et al*. (2005). Hepatocyte growth factor gene transfer to alveolar septa for effective suppression of lung fibrosis. Mol. Ther. *12*, 58–67.

Wynn, T. A. (2008). Cellular and molecular mechanisms of fibrosis. J. Pathol. *214*, 199–210.

Xiao, G. H., Jeffers, M., Bellacosa, A., Mitsuuchi, Y., Vande Woude, G. F., and Testa, J. R. (2001). Anti-apoptotic signaling by hepatocyte growth factor/Met via the phosphatidylinositol 3-kinase/Akt and mitogen-activated protein kinase pathways. Proc. Natl. Acad. Sci. USA *98*, 247–252.

Yaekashiwa, M., Nakayama, S., Ohnuma, K., Sakai, T., Abe, T., Satoh, K., Matsumoto, K., Nakamura, T., Takahashi, T., and Nukiwa, T. (1997). Simultaneous or delayed administration of hepatocyte growth factor equally represses the fibrotic changes in murine lung injury induced by bleomycin. A morphologic study. Am. J. Respir. Crit. Care Med. *156*, 1937–1944.

Zhang, J., Tsaprailis, G., and Bowden, G. T. (2008a). Nucleolin stabilizes Bcl-X L messenger RNA in response to UVA irradiation. Cancer Res. *68*, 1046–1054.

Zhang, J., Yang, J., and Liu, Y. (2008b). Role of Bcl-x_L induction in HGF-mediated renal epithelial cell survival after oxidant stress. Int. J. Clin. Exp. Pathol. *1*, 242–253.

Zhang, Y. W., and Vande Woude, G. F. (2003). HGF/SF-met signaling in the control of branching morphogenesis and invasion. J. Cell. Biochem. *88*, 408–417.